

Local Stability of PD Controlled Bipedal Walking Robots [★]

Shishir Kolathaya ^a

^aCenter for Cyber Physical Systems, Indian Institute of Science, Bengaluru, Karnataka, India

Abstract

We establish stability results for PD tracking control laws in bipedal walking robots. Stability of PD control laws for continuous robotic systems is an established result, and we extend this for hybrid robotic systems, an alternating sequence of continuous and discrete events. Bipedal robots have the leg-swing as the continuous event, and the foot-strike as the discrete event. In addition, bipeds largely have underactuations due to the interactions between feet and ground. For each continuous event, we establish that the convergence rate of the tracking error can be regulated via appropriate tuning of the PD gains; and for each discrete event, we establish that this convergence rate sufficiently overcomes the nonlinear impacts by assumptions on the hybrid zero dynamics. The main contributions are 1) Extension of the stability results of PD control laws for underactuated robotic systems, and 2) Exponential ultimate boundedness of hybrid periodic orbits under the assumption of exponential stability of their projections to the hybrid zero dynamics. Towards the end, we will validate these results in a 2-link bipedal walker in simulation.

Key words: PD controllers; Walking; Robotics; Periodic motion.

1 Introduction

Despite great advances in the theory of nonlinear controls, when it comes to practical implementation, PD control laws undisputably continue to be the most popular choice. [33, Table 1A] shows a detailed account on the list of controllers used and their corresponding acceptance ratings. The popularity of this type of control laws arises from its ease of implementation and robustness due to its model independent nature. This popularity has equally pervaded robotic systems. In fact, there are formal guarantees of stability for a broad class of robots that includes manipulators [21,36]. See Table 1, which shows a list of stability results. A more detailed list of these types of control laws and the corresponding stability results are given in [5, Table 1.1].

Despite the increase in complexity of the models, PD control laws have dominated even the domain of bipedal robots. Bipedal locomotion is hybrid in nature, with alternating phases of continuous (swinging forward of the nonstance foot) and discrete events (instantaneous impact of the nonstance foot with ground). In addition, unlike the

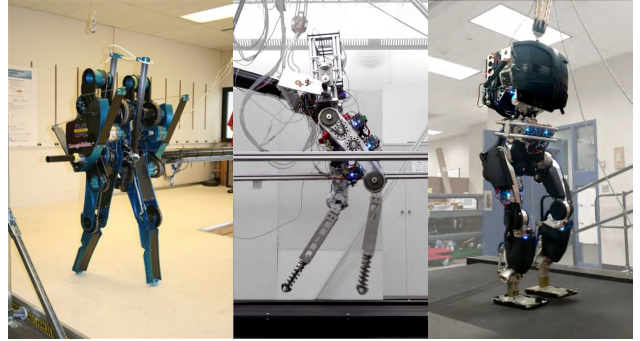


Fig. 1. Figure showing the MABEL walking robot [8] (left), DURUS-2D running robot [26] (middle), and the DURUS walking robot [24,32] (right). All of these bipeds used PD control laws for tracking reference trajectories at the low level.

PD regulation	GAS [17,34] LES [2,18], GES [20]
PD tracking	LES [15,19,36,38]

Table 1

Table showing some of the formal stability results for PD and PD based control laws for robotic systems. The abbreviations are given as follows: GAS: globally asymptotically stable, LES: locally exponentially stable, GES: globally exponentially stable.

[★] This work is supported by the DST INSPIRE Faculty Fellowship IFA17-ENG212 and the Robert Bosch Center for Cyber Physical Systems. Shishir Kolathaya is an INSPIRE Faculty Fellow at the Center for Cyber Physical Systems, Indian Institute of Science, Bengaluru. Corresponding author Shishir Kolathaya. Tel. +91 80 2360 0644.

Email address: shishirk@iisc.ac.in (Shishir Kolathaya).

industrial robotic arms, which have a fixed base, bipedal robots are largely underactuated. Fig. 1 shows some examples of bipedal robots that used PD and PD based tracking

control laws. It is worth noting that the reference trajectories that were tracked were obtained offline. In fact, the field of locomotion has largely focused on experimental realization by dividing the problem into two parts. First, obtain reference trajectories/gaits in a simulation model by using offline optimization tools [11,31]. Second, play these trajectories in the robot by a low level tracking control law [12,32,40]. Due to uncertainties in the system, model based controllers were generally avoided, thereby giving preference to the more traditional PD based control laws. These control laws are known to be “hassle free”, since they are model-independent and easy to implement. Therefore, the main goal of this paper is to explore the stability properties of PD control laws for walking robots, which include varying levels of complexity due to the presence of impacts and underactuations.

We will be establishing stability of PD control laws by the construction of strict Lyapunov functions developed by Arimoto et. al. [2], Koditschek [18], and Bayard and Wen [36] all in the same period of time 1984-1988. Local and global stability results were shown for both stationary and time varying desired configurations [15,19,38], but only for fully actuated systems. For underactuated systems, we can apply a tracking control law for the actuated states of the robot, but this does not necessarily guarantee stability, due to the coupling between the controllable and uncontrollable dynamics of the robot. In addition, the impacts due to foot-strike largely have “destabilizing” effects on the tracking errors. On the other hand, if we make assumptions about the uncontrolled dynamics of the robot i.e., existence of stable periodic orbits in the hybrid zero dynamics (HZD), we can then establish local stability results. This will be the main approach of the paper.

It is important to discuss the notion of hybrid zero dynamics (HZD) in the context of bipedal walking. HZD was introduced as a feedback design method to move beyond the traditional quasi-static flat-footed walking gaits [7,37]. The goal was to realize a stable walking gait (periodic orbit) via stabilization of a subset of the states of the robot, while the remaining states of the system exhibit uncontrolled dynamics (resulting in HZD). It was shown in [37] that if there is an exponentially stable periodic orbit in the HZD, then by employing a suitable output stabilizing control law [1,28], the periodic orbit of the full hybrid dynamics can be stabilized, resulting in stable walking.

There were two main output stabilizing controllers proposed over the last ten years using this notion of HZD—feedback linearization [28] and control Lyapunov functions (CLF) [1,24]. Both of these control methodologies relied on using a user defined ϵ , which was, in principle, increasing the controller gain. With a sufficiently large gain, the destabilizing impact events were overcome by faster convergences of the outputs. Our focus in this paper is to realize the same behavior via PD based output stabilizing control laws, wherein the desirable convergence rates are obtained via tuning of the PD gains.

Despite their widespread use in practical robotic systems, PD control laws do not have all of the properties that are typically “taken for granted” with model based control laws. Closed loop dynamics obtained from PD control laws do not necessarily have equilibrium points. This also implies that orbits in the HZD may not necessarily be orbits in the full order dynamics. However, we can use properties of the inertia, Coriolis-centrifugal and gravity matrices, and then guarantee desirable convergence rates to an ultimate bound, i.e., exponential ultimate boundedness of the outputs. This property was utilized in [38] to establish boundedness of tracking errors for fully actuated systems.

Organization. The paper is structured as follows. Section 2 introduces the hybrid system model of locomotion and the associated control methodologies. This section also describes the concept of HZD and the associated stable periodic orbit. In Section 3, we focus on underactuation and construct the PD control law for output stabilization. We will also list a set of assumptions on the desired trajectories that will be useful to simplify the main results of the paper. Section 4 contains the main results, i.e., stability results of PD based control laws for hybrid systems with Lagrangian dynamics in a series of Lemmas and Theorems. Proofs are provided in Section 5. Finally Section 6 provides the simulation results of PD control on a 2-DOF walker.

2 Robot walking model and control

In this section, we will discuss the hybrid model of a walking robot, and the associated notion of hybrid zero dynamics (HZD) for walking. The associated periodic orbits of the HZD will also be described.

Notation. \mathbb{R} is the set of real numbers, \mathbb{R}^n denotes the Euclidean space of dimension n . The open ball of radius $r > 0$ centered at $x \in \mathbb{R}^n$ is denoted by $\mathbb{B}_r(x)$. Given $x \in \mathbb{R}^n$, $|x|$ is the Euclidean norm of x , and given a matrix $A \in \mathbb{R}^{n \times m}$, $\|A\|$ is the matrix norm of A . Given a set $S \subset \mathbb{R}^n$, we denote the shortest distance between the point $x \in \mathbb{R}^n$ and the set S to be $\|x\|_S := \inf_{y \in S} \|x - y\|$. We will sometimes denote the vector $\begin{bmatrix} x^T, y^T \end{bmatrix}^T \in \mathbb{R}^{n_x + n_y}$ as the pair (x, y) . Note that the Euclidean norm has the property $|(x, y)|^2 = |x|^2 + |y|^2$.

2.1 Robot model

We consider an n -DOF robotic system, with the configuration manifold Q . We will specifically consider relative degree two systems for convenience. Therefore, we denote the state by $x = (q, \dot{q}) \in TQ$. We will denote the torque input by $u \in \mathbb{R}^m$, which is of dimension m . The dynamic model of walking consists of a continuous (swing) phase and a discrete (impact or foot-strike) phase. The discrete phase consists of a switch based on a guard condition (i.e., the swinging foot height h crossing zero). Each of these events will be described briefly below.

Continuous dynamics. Given the states (q, \dot{q}) and inputs u , the Euler-Lagrangian dynamics is given by

$$D(q)\ddot{q} + C(q, \dot{q})\dot{q} + G(q) = Bu, \quad (1)$$

where $D(q) \in \mathbb{R}^{n \times n}$ is the inertia matrix, $C(q, \dot{q}) \in \mathbb{R}^{n \times n}$ is the Coriolis-centrifugal matrix, $G(q) \in \mathbb{R}^n$ is the gravity vector, and $B \in \mathbb{R}^{n \times m}$ is the mapping of the torques to the joints. Without loss of generality, we assume that the choice of q is such that the mapping of torques to actuated joints is one-to-one i.e., each column of B consists of only one element with value one and the rest are zeros. Having described (1), we have the following properties of the model [6,9,29]¹:

Property 1 D is positive definite symmetric, and $\dot{D} - 2C$ is skew-symmetric for any $(q, \dot{q}) \in TQ$.

Property 2 There exist positive constants $c_l, c_u > 0$ such that for any $(q, \dot{q}) \in TQ$,

- $c_l \leq \|D(q)\| \leq c_u$
- $c_l \leq \|D^{-1}(q)\| \leq c_u$
- $\|\dot{D}(q)\| \leq c_u|\dot{q}|$
- $\|C(q, \dot{q})\| \leq c_u|\dot{q}|$
- $\|G(q)\| \leq c_u$.

Note that each of the matrices, D, D^{-1}, C, G have their own bounds. We have used the same constants for ease of notations. (1) can be represented in statespace form as

$$\dot{x} = f(x) + g(x)u, \quad (2)$$

by appropriate determination of f, g (see [23, (13)]). The continuous dynamics of the robot is defined on the set of admissible states $\mathbb{D} \subset TQ$, defined by

$$\mathbb{D} = \{(q, \dot{q}) \in TQ : h(q, \dot{q}) \geq 0\}, \quad (3)$$

where $h : TQ \rightarrow \mathbb{R}$ is the height of the swing foot (see Fig. 2). \mathbb{D} is called the domain. Note that h is chosen such that it only depends on the configuration q i.e., $\frac{\partial h}{\partial \dot{q}} \equiv 0$ ².

Discrete dynamics. Having described the continuous dynamics in statespace form (2), we can now describe the discrete dynamics of the walking robot. As observed in Fig. 2, when the height h crosses zero transversally, we have an impact. This impact is represented with the rigid contact model

¹ The class of robots that satisfy these properties are described in [6,9]. For example, this is true for serial manipulators with all of their prismatic joints preceding the revolute joints. Even for the prismatic joints, like in spring deflections, we know that these deflections are usually restricted by hardstops. This allows us to include a larger class of mechanical systems.

² In previous works, like in [1], h is chosen such that $L_g h \equiv 0$. This includes a larger class of h , the analysis for which is beyond the scope of this paper.

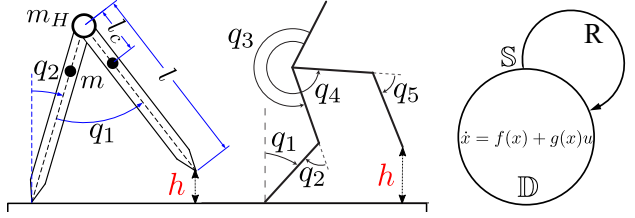


Fig. 2. Figure showing a 2-link (left) and a 5-link walking robot (middle). One foot is in contact with ground while the other is at a height h from the ground. A directed graph structure for a hybrid system model of walking is shown on the right.

of [13,14]. The swinging foot is assumed to have no rebound or slip during an impact. The velocity component of the robot state experiences a jump, while the configuration component remains continuous. Since the walking is symmetric, the roles of the legs are swapped after every foot-strike. We define the guard set representing the foot-strike as

$$\mathbb{S} = \{(q, \dot{q}) \in \mathbb{D} : h(q, \dot{q}) = 0, L_f h(q, \dot{q}) < 0\}, \quad (4)$$

with $L_g h(q, \dot{q}) \equiv 0$. Here L_f, L_g are the Lie derivatives w.r.t. f, g respectively. When $x \in \mathbb{S}$, we have a discrete event:

$$x^+ = R(x), \quad x \in \mathbb{S}, \quad (5)$$

where x is the pre-impact state, x^+ is the post-impact state, and $R : \mathbb{S} \rightarrow \mathbb{D}$ is the impact map (or reset map) of the robot.

Having obtained the continuous time (2) and discrete time (5) model of walking, we obtain the hybrid control system model as

$$\mathcal{HC} = \begin{cases} \dot{x} = f(x) + g(x)u, & x \in \mathbb{D} \setminus \mathbb{S} \\ x^+ = R(x), & x \in \mathbb{S}. \end{cases} \quad (6)$$

A pictorial representation of this hybrid control system model is given in Fig. 2. Note that based on the definition of the guard set (4), we assume that $R(\mathbb{S}) \cap \mathbb{S} = \emptyset$ (to avoid consecutive jumps).

2.2 Hybrid zero dynamics

We will now mathematically describe the notion of HZD. Denote the relative degree two outputs $y : Q \rightarrow \mathbb{R}^m$ of dimension m as

$$y(q) = y^a(q) - y^d(q), \quad (7)$$

where $y^a : Q \rightarrow \mathbb{R}^m, y^d : Q \rightarrow \mathbb{R}^m$ are the actual and the desired values respectively. The desired values are chosen such that $y(q) = 0$ for at least one q , like in [37, HH4]. Similarly, denote the passive states (or the unactuated states) of dimension $2l = 2n - 2m$ as $z : TQ \rightarrow \mathbb{R}^{2l}$. Accordingly,

we have the output dynamics (or the transverse dynamics) and passive dynamics of the form:

$$\dot{y} = L_f^2 y + L_g L_f y u \quad (8)$$

$$\dot{z} = \psi(y, \dot{y}, z). \quad (9)$$

Here $\psi : \mathbb{R}^{2n} \rightarrow \mathbb{R}^{2l}$ is the vector field (of z). Note that z is chosen such that $L_g z \equiv 0$ and a diffeomorphism from (q, \dot{q}) to (y, \dot{y}, z) exists (see Assumption 2 further ahead). We denote this diffeomorphism as $\Phi : \mathbb{D} \rightarrow \mathbb{R}^{2n}$.

With a suitable output stabilizing controller, we can guarantee convergence of the outputs (y, \dot{y}) to zero. For example, a feedback linearizing control law of the form:

$$u_{IO} = L_g L_f y^{-1} (-L_f^2 y - 2\varepsilon \dot{y} - \varepsilon^2 y), \quad (10)$$

yields exponential convergence of the outputs to zero. If $(y, \dot{y}) = (0, 0)$, the resulting passive dynamics given by

$$\dot{z} = \psi(0, 0, z), \quad (11)$$

is now called the zero dynamics of the closed loop system of (1). It is important to note that output stabilization can be realized only during the swing mode (continuous event) of the hybrid dynamics. On the other hand, if the outputs are chosen in such a way that the zero dynamics is invariant of the discrete dynamics, we have *hybrid zero dynamics* (HZD). Consider the reduced dimensional surface:

$$\mathbb{Z} = \{(q, \dot{q}) \in \mathbb{D} : y(q) = 0, \dot{y}(q, \dot{q}) = 0\}. \quad (12)$$

Also consider a post-impact map defined in terms of the transformed coordinates:

$$\Delta(y, \dot{y}, z) := \Phi \circ R \circ \Phi^{-1}(y, \dot{y}, z), \quad (13)$$

which consists of two components:

$$\begin{bmatrix} \Delta_y(y, \dot{y}, z) \\ \Delta_z(y, \dot{y}, z) \end{bmatrix} := \Delta(y, \dot{y}, z), \quad (14)$$

corresponding to the outputs (y, \dot{y}) and the zero coordinates z respectively. We have HZD, if the following is satisfied:

$$R(\mathbb{S} \cap \mathbb{Z}) \subset \mathbb{Z} \quad \text{or} \quad \Delta(\Phi(\mathbb{S} \cap \mathbb{Z})) \subset \Phi(\mathbb{Z}). \quad (15)$$

With this formulation, the goal now is to obtain a periodic orbit in the HZD and, consequently, a periodic orbit in the full order hybrid dynamics.

2.3 Hybrid periodic orbits

With the initial condition $(y^*, \dot{y}^*, z^*) \in \Phi(\mathbb{S})$, and the control law (10), let $\varphi_t(\Delta(y^*, \dot{y}^*, z^*))$ be the resulting flow of (8),

(9) represented in transformed coordinates. By assuming right continuity [35, Section II-B], this flow is, in fact, the solution for the entire hybrid system (6) that includes both the continuous and the discrete dynamics. We say that there is a periodic orbit if there exists a $T^* > 0$ such that

$$\lim_{t \rightarrow T^*} \varphi_t(\Delta(y^*, \dot{y}^*, z^*)) = (y^*, \dot{y}^*, z^*), \quad (16)$$

and the point (y^*, \dot{y}^*, z^*) is called the fixed point of the periodic orbit. We will denote this periodic orbit as

$$\mathcal{O} := \{\varphi_t(\Delta(y^*, \dot{y}^*, z^*)) \in \Phi(\mathbb{D}) : 0 \leq t < T^*\}. \quad (17)$$

We will also denote the fixed point in angle-velocity coordinates as $x^* := \Phi^{-1}(y^*, \dot{y}^*, z^*)$.

If the periodic orbit \mathcal{O} satisfies some properties (like transversality and isolated intersections with the guard $\Phi(\mathbb{S})$ [28, H2.4, H2.5], [35, A.6, A.7]), then we know that for an initial state x_0 in a small enough neighborhood of x^* i.e., $x_0 \in \mathbb{B}_r(x^*) \cap \mathbb{S}$, the time-to-impact function is well defined with distinct lower and upper bounds, and can be obtained as

$$T(y, \dot{y}, z) := \inf\{t > 0 : h(\Phi^{-1}(\varphi_t(\Delta(y, \dot{y}, z)))) = 0\}, \quad (18)$$

where $(y, \dot{y}, z) = \Phi(x_0)$. See [28, 35] for more details on time-to-impact or dwell-time functions. Note that the problem formulation is constructed in such a way that undesirable behaviors like consecutive jumps and Zeno executions are avoided. Later on (Lemma 1, 2), we will show that by using sufficiently large controller gains, even PD based control laws yield well defined time-to-impact functions.

Having defined the periodic orbit and time-to-impact functions, we can define some stability properties for \mathcal{O} that will be useful throughout the paper. For the following definition, we consider the solution φ_t for the entire time interval $[0, \infty)$ (by assuming right continuity [35, Section II-B]).

Definition 1 \mathcal{O} is said to be locally exponentially stable (LES) if there are constants $M, r, \lambda > 0$ such that for all $(y, \dot{y}, z) \in \mathbb{B}_r(0, 0, z^*) \cap \Phi(\mathbb{S})$,

$$\|\varphi_t(\Delta(y, \dot{y}, z))\|_{\mathcal{O}} \leq M e^{-\lambda t} \|\Delta(y, \dot{y}, z)\|_{\mathcal{O}}. \quad (19)$$

Similarly, \mathcal{O} is said to be locally exponentially ultimately bounded (LEUB) if there are constants $M, r, \lambda, d > 0$ such that for all $(y, \dot{y}, z) \in \mathbb{B}_r(0, 0, z^*) \cap \Phi(\mathbb{S})$,

$$\|\varphi_t(\Delta(y, \dot{y}, z))\|_{\mathcal{O}} \leq M e^{-\lambda t} \|\Delta(y, \dot{y}, z)\|_{\mathcal{O}} + d. \quad (20)$$

We will be mainly establishing LEUB of \mathcal{O} via Poincaré maps (due to equivalence in stability results between periodic orbits and Poincaré maps [28, 35]). Therefore, it is sufficient if we define the flow φ for the closed interval $[0, T]$, i.e., for only the continuous dynamics. After every impact,

the time t can be reset to zero with the resulting new initial state on the Poincaré section. More details on Poincaré maps are provided in Section 4.

Remark 1 *The notion of ultimate boundedness is valid even for systems without equilibrium points including periodic orbits [16, 4.8]. In the analysis that follows the next section, we will show that the set of points \mathcal{O} can be shown to be ultimately bounded when PD based control laws are applied.*

We can have similar notions of ultimate boundedness for the output coordinates in the continuous dynamics. For convenience, we will denote the initial state as (y_0, \dot{y}_0, z_0) and the resulting trajectory, post-impact, as $(y(t), \dot{y}(t), z(t))$ with $(y(0), \dot{y}(0), z(0)) = \Delta(y_0, \dot{y}_0, z_0)$. We have the following definition for boundedness of the outputs:

Definition 2 *Given $T_\delta > 0$, the zero values of the outputs $(y(t), \dot{y}(t))$ are said to be locally exponentially ultimately bounded (LEUB) in the interval $t \in [0, T_\delta]$ if there are constants $M, r, \lambda, d > 0$ such that for all $(y_0, \dot{y}_0, z_0) \in \mathbb{B}_r(0, 0, z^*) \cap \Phi(S)$,*

$$|(y(t), \dot{y}(t))| \leq Me^{-\lambda t} |(y(0), \dot{y}(0))| + d. \quad (21)$$

The notion of ultimate boundedness (UB) and local exponential ultimate boundedness (LEUB) are applied to systems that are forward complete, i.e., $t \in [0, \infty)$. We would still like to use this definition for shorter finite intervals, since we have a hybrid system with restrictions on dwell-time. Therefore, whenever we say that the outputs are LEUB in the interval $[0, T_\delta]$, we mean that (21) is valid for $[0, T_\delta]$.

It was shown in [1, Theorem 2] that if there is an exponentially stable periodic orbit in the HZD, then by choosing a sufficiently large enough ε in (10), we can realize an exponentially stable periodic orbit in the full order dynamics. In this paper, we will particularly focus on obtaining a similar result (boundedness) with PD control by choosing large enough gains.

3 PD tracking with underactuation

In this section, we will focus on PD based control laws for robotic systems with underactuation. Since m is the degree of actuation (DOA) and n is the degree of freedom (DOF), we have the corresponding degree of underactuation as $l = n - m$. Accordingly, we have the following separation in the dynamics:

$$\begin{aligned} D_{11}(q)\ddot{q}^u + D_{12}(q)\ddot{q}^a + C_1(q, \dot{q})\dot{q} + G_1(q) &= 0 \\ D_{21}(q)\ddot{q}^u + D_{22}(q)\ddot{q}^a + C_2(q, \dot{q})\dot{q} + G_2(q) &= u, \end{aligned} \quad (22)$$

where the terms corresponding to D, C, G are apparent from the setup. q^u, q^a are the unactuated and actuated configurations respectively. Also let $B_c \in \mathbb{R}^{n \times l}$ be the constant matrix

obtained in such a way that if the l unactuated joints had inputs, then these inputs would be mapped via this matrix. In other words, the new notations B_c, q^u, q^a are defined in such a way that

$$q = \begin{bmatrix} B_c & B \end{bmatrix} \begin{bmatrix} q^u \\ q^a \end{bmatrix}. \quad (23)$$

Accordingly, we have that

$$\begin{aligned} \begin{bmatrix} D_{11} & D_{12} \\ D_{21} & D_{22} \end{bmatrix} &= \begin{bmatrix} B_c^T D B_c & B_c^T D B \\ B^T D B_c & B^T D B \end{bmatrix} \\ \begin{bmatrix} C_1 \\ C_2 \end{bmatrix} &= \begin{bmatrix} B_c^T C \\ B^T C \end{bmatrix} \\ \begin{bmatrix} G_1 \\ G_2 \end{bmatrix} &= \begin{bmatrix} B_c^T G \\ B^T G \end{bmatrix}. \end{aligned} \quad (24)$$

The matrices B_c, B have some important properties that will be utilized in the proofs in this section. Some of them are

$$[B_c, B] = \begin{bmatrix} B_c^T \\ B^T \end{bmatrix} = \mathbf{1}_{n \times n}$$

$$B^T B = \mathbf{1}_{m \times m}, \quad B_c^T B_c = \mathbf{1}_{l \times l}, \quad B_c^T B = \mathbf{0}_{l \times m}, \quad B^T B_c = \mathbf{0}_{m \times l},$$

where $\mathbf{1}$ is the identity matrix, $\mathbf{0}$ is the zero matrix with appropriate dimensions. Based on these properties \ddot{q}^u can be eliminated from (22) to obtain

$$B^T A D B \ddot{q}^a + B^T A C \dot{q} + B^T A G = u, \quad (25)$$

where

$$A := \mathbf{1}_{n \times n} - D B_c (B_c^T D B_c)^{-1} B_c^T,$$

with $\mathbf{1}_{n \times n}$ being the identity matrix of dimension n . It can be verified that $B^T A D B$ is nothing but the Schur complement of $D_{11} = B_c^T D B_c$ in D , and it has some important properties:

Proposition 1 *$B^T A(q) D(q) B$ is symmetric positive definite for all $(q, \dot{q}) \in TQ$.*

Proposition 2 *There exist positive constants c_l, c_u such that for all $(q, \dot{q}) \in TQ$,*

- $c_l \leq \|B^T A(q) D(q) B\| \leq c_u$
- $c_l \leq \|(B^T A(q) D(q) B)^{-1}\| \leq c_u$
- $\|A(q)\| \leq c_u$
- $\|A(q) D(q)\| \leq c_u$
- $\|\dot{A}(q, \dot{q}) D(q) + A(q) \dot{D}(q, \dot{q})\| \leq c_u |\dot{q}|$
- $\|B^T A(q) C(q, \dot{q})\| \leq c_u |\dot{q}|$
- $\|B^T A(q) G(q)\| \leq c_u$.

See [25, Theorem 2.1, Corollary 4.1] and [3, Appendix A.5.5] for more details on Schur complement matrices. Note that, similar to Property 2, we have used the same constants c_l, c_u for ease of notations. Proofs of Propositions 1 and 2 are provided in Appendix A.

3.1 Outputs and control

Having represented the dynamics in the form (25) by eliminating \ddot{q}^u , we will now define the outputs for the robot. For the actuated configuration q^a , we define the following relative degree two outputs:

$$e(q^a, \tau) = q^a - q_d^a(\tau), \quad (26)$$

where e defines the difference between the actual and the desired value of the actuated joints of the robot. The desired configuration $q_d^a : \mathbb{R}_{\geq 0} \rightarrow \mathbb{R}^m$ is a function of a variable called the phase (or the gait timing) variable $\tau : \mathbb{Q} \rightarrow \mathbb{R}$, which is a function of the configuration. By a slight abuse of notations, we will sometimes remove the phase τ and denote the desired trajectories by $q_d^a(q)$.

Having defined the error e , we have its derivative as

$$\dot{e}(q, \dot{q}) = \dot{q}^a - \frac{\partial q_d^a(q)}{\partial q} \dot{q} = J(q) \dot{q}^a - \frac{\partial q_d^a(q)}{\partial q^u} \dot{q}^u.$$

and $J(q) := \frac{\partial e(q)}{\partial q^a}$ is the Jacobian w.r.t. q^a . We use the following PD control law:

$$u_{PD}(q, \dot{q}) = -J(q)^T K_p e(q) - J(q)^T K_d \dot{e}(q, \dot{q}), \quad (27)$$

where K_p, K_d are the gain matrices of dimension m .

Remark 2 If the desired configuration is only a function of q^u , then $J(q) = \mathbf{1}$, which reduces (27) to the familiar form of PD control law.

For simplicity, we will assume that equal gains are applied for every joint i.e., $K_p = k_p \mathbf{1}$, $K_d = k_d \mathbf{1}$ for some $k_p, k_d > 1$ and an identity matrix $\mathbf{1}$ of appropriate size. Having defined this PD control law (27), we have the resulting closed loop dynamics of (6) as

$$\dot{x} = f^{cl}(x) := f(x) + g(x) u_{PD}(q, \dot{q}), \quad (28)$$

and with the initial state $x_0 \in \mathbb{S}$, we have the resulting flow (integral curve) of the continuous dynamics as $x(t) = (q(t), \dot{q}(t))$, where $(q(0), \dot{q}(0)) = R(x_0)$ and $t \in [0, T]$ with $T > 0$ (see (18)) being the time until the next impact.

3.2 Hybrid zero dynamics

For underactuated robotic systems, we typically choose the zero coordinates to be the following:

$$z(q, \dot{q}) := \begin{bmatrix} z_1(q) \\ z_2(q, \dot{q}) \end{bmatrix} := \begin{bmatrix} q^u \\ B_c^T D(q) \dot{q} \end{bmatrix}. \quad (29)$$

It is important to note that the coordinates z shown above are chosen based on e (see Assumption 2 ahead). Accordingly, we have the output zero coordinates as (e, \dot{e}, z) , and the corresponding transformation as $\Phi(q, \dot{q}) = (e, \dot{e}, z)$. With this transformation, we have the following passive dynamics:

$$\begin{aligned} \dot{z} &= \psi(\Phi(q, \dot{q})), & (q, \dot{q}) &\in \mathbb{D} \setminus \mathbb{S} \\ z^+ &= \Delta_z(\Phi(q, \dot{q})), & (q, \dot{q}) &\in \mathbb{S}, \end{aligned} \quad (30)$$

where ψ is given by

$$\psi(\Phi(q, \dot{q})) := \begin{bmatrix} \dot{q}^u \\ B_c^T (\dot{D}(q, \dot{q}) \dot{q} - C(q, \dot{q}) \dot{q} - G(q)) \end{bmatrix}. \quad (31)$$

Here the input u will not appear due to underactuation. If the outputs are zero i.e., $(e, \dot{e}) = (0, 0)$, and if the hybrid invariance conditions (15) are satisfied (with the notations y, \dot{y} replaced with e, \dot{e}), we have hybrid zero dynamics (HZD). The HZD obtained lies on the reduced dimensional surface:

$$\mathbb{Z} = \{(q, \dot{q}) \in \mathbb{D} : e(q) = 0, \dot{e}(q, \dot{q}) = 0\}. \quad (32)$$

Stability of HZD has been extensively studied, where the desired values q_d^a , and the phase $\tau(q)$ are chosen in such a way that the HZD has an exponentially stable periodic orbit [7, 10, 37]. Therefore, given that there is a constructive way to realize an exponentially stable periodic orbit in the HZD, we make the following assumption:

Assumption 1 The hybrid zero dynamics given by

$$\mathcal{X} := \begin{cases} \dot{z} = \psi(0, 0, z), & (0, 0, z) \in \Phi(\mathbb{Z} \setminus (\mathbb{Z} \cap \mathbb{S})) \\ z^+ = \Delta_z(0, 0, z), & (0, 0, z) \in \Phi(\mathbb{Z} \cap \mathbb{S}) \end{cases}, \quad (33)$$

has an exponentially stable periodic orbit, \mathcal{O}_z , transverse to $\Phi(\mathbb{Z} \cap \mathbb{S})$.

Remark 3 Periodic orbits on the HZD are usually obtained through an offline optimization problem [11]. Since the model is not accurately known, Assumption 1 may seem restrictive. Relaxation of the above assumption with uncertainties incorporated have been studied in [22], where the periodic orbit was shown to be exponentially ultimately bounded. In order to keep focus on the stability analysis for PD control laws, we will continue to use Assumption 1 for the rest of the paper.

Denote the integral curve of the continuous zero dynamics as $\varphi_t^{\text{HZD}} : \mathbb{R}^{2l} \rightarrow \mathbb{R}^{2l}$. Since the HZD has a periodic orbit, we have a fixed point z^* , and the associated period T^* that satisfies: $\varphi_{T^*}^{\text{HZD}}(\Delta_z(0, 0, z^*)) = z^*$. We have this periodic orbit defined as

$$\mathcal{O}_z = \{\varphi_t^{\text{HZD}}(\Delta_z(0, 0, z^*)) \in \mathbb{R}^{2l} : 0 \leq t < T^*\}. \quad (34)$$

3.3 Exponential stability via Poincaré maps

Exponential stability of periodic orbits is characterized by using Poincaré maps [28,35]. Therefore, we define the following Poincaré map:

$$\rho(z_s) := \varphi_{T_p(z_s)}^{\text{HZD}}(\Delta_z(0, 0, z_s)). \quad (35)$$

Here $(0, 0, z_s) \in \Phi(\mathbb{Z} \cap \mathbb{S})$ is the initial state, and T_p is the reduced time-to-impact function given by

$$T_p(z_s) = \inf\{t > 0 : h(\Phi^{-1}(\iota(\varphi_t^{\text{HZD}}(\Delta_z(0, 0, z_s)))) = 0\}, \quad (36)$$

obtained similar to (18). Note that we have used the subscript s in z_s to distinguish it from the evolution of z of the full order dynamics. Since \mathcal{O}_z is exponentially stable, by the converse Lyapunov theorem for discrete systems, there exists an exponentially convergent Lyapunov function V_z for some $r > 0$, and positive constants c_1, c_2, c_3, c_4 such that for all $z_s \in \mathbb{B}_r(z^*) \cap (\mathbb{Z} \cap \mathbb{S})$,

$$\begin{aligned} c_1 |z_s - z^*|^2 &\leq V_z(z_s - z^*) \leq c_2 |z_s - z^*|^2 \\ V_z(\rho(z_s) - z^*) - V_z(z_s - z^*) &\leq -c_3 |z_s - z^*|^2 \\ |V_z(z_s - z^*) - V_z(z'_s - z^*)| &\leq c_4 |z_s - z'_s| \cdot (|z_s - z^*| + |z'_s - z^*|). \end{aligned} \quad (37)$$

In addition, we know that there exist constants $c_5 > 0$, $\gamma \in (0, 1)$ such that

$$|\rho^i(z_s) - z^*| \leq c_5 \gamma^i |z_s - z^*|. \quad (38)$$

We will be mainly using this property along with the Poincaré map of the full order hybrid system (described in the next section) to establish our main results.

3.4 Hybrid dynamics

We can reconstruct \mathcal{O} from \mathcal{O}_z by the canonical embedding $\iota(z) := (0, 0, z)$, i.e., $\mathcal{O} = \iota(\mathcal{O}_z)$. Since \mathcal{O} is not necessarily an orbit of the full order hybrid system, we will denote the point: $(0, 0, z^*)$, simply as a nominal point of \mathcal{O} . Given that \mathcal{O}_z is exponentially stable, we are interested in the stability properties of \mathcal{O} when a PD control law of the form (27) is applied. Accordingly, we have the following hybrid dynamics

expressed in terms of the transformed coordinates (e, \dot{e}, z) :

$$\mathcal{H} = \begin{cases} \ddot{e} &= f_e(e, \dot{e}, z) \\ &+ g_e(e, \dot{e}, z) u_{\text{PD}}(\Phi^{-1}(e, \dot{e}, z)) \\ \dot{z} &= \psi(e, \dot{e}, z), \\ &\text{when } (e, \dot{e}, z) \in \Phi(\mathbb{D} \setminus \mathbb{S}) \\ (e^+, \dot{e}^+, z^+) &= \Delta(e, \dot{e}, z), \\ &\text{when } (e, \dot{e}, z) \in \Phi(\mathbb{S}) \end{cases}, \quad (39)$$

where f_e, g_e are obtained from the Lie derivatives of e . For the continuous dynamics in (39), we will use $e(t), \dot{e}(t), z(t)$ in place of the flow φ for convenience. The value at $t = 0$, i.e., $(e(0), \dot{e}(0), z(0))$, are the post-impact states of the initial state $(e_0, \dot{e}_0, z_0) := \Phi(x_0)$. We will also denote the trajectory on the orbit \mathcal{O} by $(q^*(t), \dot{q}^*(t))$, and in the transformed coordinates by $(0, 0, z^*(t))$. The following additional assumptions are used to establish the main result.

3.5 Additional assumptions on \mathcal{O}_z and the outputs e

We make the following assumptions on e . In particular, these assumptions are for a local configuration space of q , i.e., we will pick a tube of radius r around the orbit $q^*(t)$:

$$\mathbb{N}_r = \{q \in \mathbb{Q} : \inf_{t \in [0, T]} \|q - q^*(t)\| \leq r\}. \quad (40)$$

We have the following first assumption on the outputs e (26):

Assumption 2 The transformation $(q^\mu, e(q)) : \mathbb{Q} \rightarrow \mathbb{R}^n$ is a local diffeomorphism onto its image for every $q \in \mathbb{N}_r$.

By Assumption 2, the Jacobian w.r.t. q is nonsingular:

$$J_e(q) := \begin{bmatrix} \mathbf{1}_{l \times l} & \mathbf{0}_{l \times m} \\ \frac{\partial e(q)}{\partial q^\mu} & J(q) \end{bmatrix}. \quad (41)$$

As a result, the continuous dynamics (1) can be reformulated and represented in terms of q^μ, e as

$$D_e(q) \begin{bmatrix} \ddot{q}^\mu \\ \ddot{e} \end{bmatrix} + C_e(q, \dot{q}) \begin{bmatrix} \dot{q}^\mu \\ \dot{e} \end{bmatrix} + G_e(q) = J_e^{-T}(q) B u, \quad (42)$$

where $D_e = J_e^{-T} D J_e^{-1}$, $C_e = J_e^{-T} C J_e^{-1} + J_e^{-T} D \frac{d(J_e^{-1})}{dt}$, $G_e = J_e^{-T} G$. As a result of this change of variables, the following

functions will appear frequently throughout the paper:

$$\begin{aligned} A_e(q) &:= \mathbf{1}_{n \times n} - D_e(q)B_c(B_c^T D_e(q)B_c)^{-1}B_c^T \\ B_e(q) &:= \mathbf{1}_{m \times m} + B^T D_e(q)B_c(B_c^T D_e(q)B_c)^{-1} \frac{\partial e(q)}{\partial q^u}^T \\ B'_e(q) &:= \mathbf{1}_{l \times l} - (B_c^T D(q)B_c)^{-1}B_c^T D(q)B J^{-1}(q) \frac{\partial e(q)}{\partial q^u}. \end{aligned} \quad (43)$$

Similar to (25), we can eliminate \ddot{q}^u from (42) to obtain

$$B^T A_e D_e B \ddot{e} + B^T A_e C_e \begin{bmatrix} \dot{q}^u \\ \dot{e} \end{bmatrix} + B^T A_e G_e = B_e J^{-T} u, \quad (44)$$

where A_e, B_e are obtained from (43). Having defined A_e, B_e , we now impose the following assumption:

Assumption 3 *The outputs e are chosen such that the norm $\|\frac{\partial e(q)}{\partial q^u}\|$ is sufficiently small. In particular, this norm is chosen such that for all $(q, \dot{q}) \in \bigcup_{q \in \mathbb{N}_r} T_q \mathbb{Q}$,*

1. B'_e is invertible, and
2. $\Lambda_{B_e} := \begin{bmatrix} B_e + B_e^T & B_e + (1 + |e|)(B_e^T - \mathbf{1}) \\ B_e^T + (1 + |e|)(B_e - \mathbf{1}) & (1 + |e|)(B_e + B_e^T) \end{bmatrix}$ is symmetric positive definite.

where B'_e, B_e are dependent on q (given by (43)).

Assumption 3 only requires that e has small variations w.r.t. q^u . This will be verified with the example biped model in Section 6. We choose e such that the entries of $B_e - \mathbf{1}_{m \times m}, B'_e - \mathbf{1}_{l \times l}$ are small in magnitude. By Gershgorin's circle theorem [4, Theorem 2.1], the diagonal entries of B'_e, B_e are positive and dominate the off-diagonal entries, thereby rendering them invertible. Furthermore, since Λ_{B_e} is symmetric, the eigenvalues are real and positive, thereby ensuring positive definiteness. Note that this assumption is sufficient but not necessary, and its relaxed formulations are possible, which will be a subject of future work.

Since the norm is a continuous function, $\|J_e(q)\|$ has nonzero upper and lower bounds on a compact set \mathbb{N}_r . We can make use of this property to establish the following:

Proposition 3 *D_e is symmetric positive definite, and $\dot{D}_e - 2C_e$ is skew-symmetric. In addition, there exist $c_l, c_u > 0$ (possibly smaller, larger than previously determined c_l, c_u) such that for any $(q, \dot{q}) \in \bigcup_{q \in \mathbb{N}_r} T_q \mathbb{Q}$,*

1. $c_l \leq \|D_e(q)\| \leq c_u$
2. $c_l \leq \|D_e^{-1}(q)\| \leq c_u$
3. $\|\dot{D}_e(q)\| \leq c_u(|\dot{q}^u| + |\dot{e}|)$
4. $\|C_e(q, \dot{q})\| \leq c_u(|\dot{q}^u| + |\dot{e}|)$
5. $\|G_e(q)\| \leq c_u$.

Note that we have not restricted the tangent space $T_q \mathbb{Q}$ to a compact set. This will be useful for allowing larger velocity variations (see Remark 5 ahead). Proof of Proposition 3 is provided in Appendix B. The interested reader may also see [30, Chapter 4, Section 5.4] for more details.

Similar to Proposition 3, we have the following properties for $B^T A_e D_e B$:

Proposition 4 *$B^T A_e D_e B$ is symmetric positive definite. In addition, there exist positive constants $c_l, c_u > 0$ such that for all $(q, \dot{q}) \in \bigcup_{q \in \mathbb{N}} T_q \mathbb{Q}$,*

- $c_l \leq \|B^T A_e(q) D_e(q) B\| \leq c_u$
- $c_l \leq \|(B^T A_e(q) D_e(q) B)^{-1}\| \leq c_u$
- $\|B^T \dot{A}_e(q, \dot{q}) D_e(q) B + B^T A_e(q) \dot{D}_e(q, \dot{q}) B\| \leq c_u(|\dot{q}^u| + |\dot{e}|)$
- $\|B^T A_e(q) C_e(q, \dot{q})\| \leq c_u(|\dot{q}^u| + |\dot{e}|)$
- $\|B^T A_e(q) G_e(q)\| \leq c_u$.

Proof is provided in Appendix C. With these propositions, we are now ready to present the main results of the paper.

4 Main results

The main results will be in a series of Lemmas and Theorems. Since we are interested in a local result, we start from a small neighborhood of $(0, 0, z^*)$ i.e., $(e_0, \dot{e}_0, z_0) \in \mathbb{B}_r(0, 0, z^*) \cap \Phi(\mathbb{S})$. The neighborhood radius r may, perhaps, be smaller than previously determined. Later on, r may be reduced further depending upon the gains k_p, k_d . With this initial condition, we have the following time-to-impact (dwell-time) function:

$$T(e_0, \dot{e}_0, z_0) := \begin{cases} \inf\{t > 0 : h(\Phi^{-1}(e(t), \dot{e}(t), z(t))) = 0\}, & \text{if } \exists t \text{ s.t. } (e(t), \dot{e}(t), z(t)) \in \Phi(\mathbb{S}) \\ \infty, & \text{otherwise,} \end{cases} \quad (45)$$

where $(e(0), \dot{e}(0), z(0)) = \Delta(e_0, \dot{e}_0, z_0)$. Since $R(\mathbb{S}) \cap \mathbb{S} = \emptyset$, we know that there is a $T_{\min} > 0$ such that $T \geq T_{\min}$ (later we will also show that upper bound for T also exists). We have the following first result. We show here that the outputs are LEUB (Definition 2).

Lemma 1 *Let the system (39) be given, and let the desired configuration q_d^a be chosen such that Assumptions 2-3 are satisfied. Then there exist sufficiently large enough gains $k_p, k_d > 1$, and a correspondingly small enough $r > 0$, $T_\delta > 0$, such that for all $(e_0, \dot{e}_0, z_0) \in \mathbb{B}_r(0, 0, z^*) \cap \Phi(\mathbb{S})$, the outputs $(e(t), \dot{e}(t))$ are LEUB in the interval $t \in [0, T_\delta]$.*

Note that [16, 3.2] establishes boundedness by Gronwall-Bellman result for any finite interval (any arbitrary T_δ) by choosing an initial point (e_0, \dot{e}_0, z_0) very close to the nominal point $(0, 0, z^*)$ (i.e., by reducing r). We cannot use this

approach due to the fact that \mathcal{O} is not necessarily an orbit for (39). On the other hand, the following Lemma will, in fact, allow us to simply pick larger k_p, k_d for stretching T_δ to T , thereby establishing ultimate boundedness of the outputs for the entire step.

Lemma 2 *Let the system (39) be given, and let the desired configuration q_d^a be chosen such that Assumptions 2-3 are satisfied. Given that \mathcal{O}_z is an orbit of the HZD, and $k_p, k_d, r, T_\delta > 0$ are chosen such that the outputs $(e(t), \dot{e}(t))$ are LEUB in the interval $[0, T_\delta]$, we then have the following:*

1. If $(e_0, \dot{e}_0, z_0) = (0, 0, z^*)$, then there exist $C_k, C_t > 0$ with C_k dependent on k_p, k_d such that

$$|z(t) - z^*(t)| \leq C_k(k_p, k_d)e^{C_t t} T_\delta, \quad t \in [0, T_\delta], \quad (46)$$

where C_k decreases with increasing k_p, k_d .

2. For every $\delta > 0$, there exist $k_p, k_d > 1$, greater than previously determined, such that

$$|T(0, 0, z^*) - T^*| < \delta. \quad (47)$$

3. There exist $k_p, k_d > 1$, greater than previously determined, and $r > 0$, such that for all $(e_0, \dot{e}_0, z_0) \in \mathbb{B}_r(0, 0, z^*) \cap \Phi(\mathbb{S})$,

$$T_{\min} \leq T(e_0, \dot{e}_0, z_0) \leq T_{\max}, \quad (48)$$

for some pre-defined constants $T_{\max} > T^* > T_{\min} > 0$.

Lemmas 1 and 2 together show that $(e(t), \dot{e}(t), z(t))$ can be close to \mathcal{O} for the entire step. The ensuing lemma and the two theorems will extend this result for the entire hybrid dynamics.

For simplicity of notation, we will denote the output coordinates as $\eta := (e, \dot{e})$, and shift z^* to zero. We will also drop the subscript 0 from the initial states η_0, z_0 ³. Since we are analyzing periodic orbits, we will be using Poincaré maps defined as

$$\mathbb{P}(\eta, z) := \varphi_{T(\eta, z)}(\Delta(\eta, z)), \quad (49)$$

where T is the time-to-impact function (45) (which is well defined based on (48)). \mathbb{P} has two components $\mathbb{P}_\eta, \mathbb{P}_z$ corresponding to the coordinates η, z respectively. We can also establish some of the properties of impact maps. We know that Δ can be separated into two components $(\Delta_\eta, \Delta_z) = \Delta$ corresponding to η and z . By local Lipschitz continuity and hybrid invariance conditions, we have the following:

$$\begin{aligned} |z(0) - z_s(0)| &= |\Delta_z(\eta, z) - \Delta_z(0, z)| \leq L_\Delta |\eta| \\ |z(0) - z^*(0)| &= |\Delta_z(\eta, z) - \Delta_z(0, 0)| \leq L_\Delta (|\eta| + |z|), \end{aligned} \quad (50)$$

³ Since the ensuing Lemma and Theorems are established via Poincaré maps, there is no confusion.

where L_Δ is the Lipschitz constant. Since $\Delta_\eta(0, z) = 0$,

$$|(e(0), \dot{e}(0))| = |\Delta_\eta(\eta, z) - \Delta_\eta(0, z)| \leq L_\Delta |\eta|. \quad (51)$$

There is an elegant relationship between the time-to-impact functions T, T_p and the Poincaré maps \mathbb{P}, ρ that can be utilized to prove the main theorem. This is given in the form of the following lemma.

Lemma 3 *Let the system (39) be given, and let the desired configuration q_d^a be chosen such that Assumptions 2-3 are satisfied. Given that \mathcal{O}_z is an LES periodic orbit of the HZD transverse to $\Phi(\mathbb{Z} \cap \mathbb{S})$, then there exist large gains k_p, k_d , small enough $r > 0$, and corresponding $C_T, C_P, d_T, d_P > 0$ such that for all $(\eta, z) \in \mathbb{B}_r(0, z^*) \cap \Phi(\mathbb{S})$,*

$$|T(\mathbb{P}(\eta, z)) - T_p(z)| \leq C_T |\eta| + d_T \quad (52)$$

$$|\mathbb{P}_z(\eta, z) - \rho(z)| \leq C_P |\eta| + d_P. \quad (53)$$

In addition, the gains k_p, k_d can be further increased and r can be further decreased in such a way that C_T, C_P remain constant and d_T, d_P decrease (with increasing k_p, k_d).

Lemmas 1-3 yield r and the PD gains k_p, k_d , which yield the inequalities (52), (53). We will now state the following well known result for periodic orbits [35]:

Theorem 1 *Given the set of points \mathcal{O} obtained from the embedding ι of the periodic orbit \mathcal{O}_z (34) of the hybrid zero dynamics \mathcal{Z} (33), the following are equivalent:*

1. $\mathcal{O} = \iota(\mathcal{O}_z)$ of the hybrid system \mathcal{H} (39) is LEUB.
2. $(0, 0) = \Phi(x^*)$ of the map \mathbb{P} (49) is LEUB.

Theorem 1 will be used to establish the main theorem of the paper that follows. We will not be proving this theorem, since it is directly obtained as a consequence of [35, Theorem 1] (by simply replacing the class \mathcal{K} function of the disturbance with a constant d). The proof of [35, Theorem 1] is for a stronger property—input-to-state stability (ISS)—and similar results can be derived for boundedness. We can establish that the ultimate bound, given by d in (20), can be decreased to an arbitrarily small value by choosing appropriate k_p, k_d . As $d \rightarrow 0$, the resulting orbit of the closed loop system coincides with \mathcal{O} . Therefore, Theorem 1 will be used to establish boundedness of periodic orbits via Poincaré maps.

Main theorem. We will now present the main theorem.

Theorem 2 *Let the system (39) be given, and let the desired configuration q_d^a be chosen such that Assumptions 2-3 are satisfied. If \mathcal{O}_z is an LES periodic orbit of the hybrid zero dynamics \mathcal{Z} (33) transverse to $\Phi(\mathbb{Z} \cap \mathbb{S})$, then for sufficiently large enough gains $k_p, k_d > 1$, \mathcal{O} is an LEUB periodic orbit of the full order hybrid dynamics \mathcal{H} (39).*

We will prove Lemmas 1-3, and also Theorem 2 in the next section.

5 Proofs of Lemmas 1-3 and Theorem 2

PROOF. [of Lemma 1] We consider the following Lyapunov candidate:

$$V_e(e, \dot{e}, q) = V_0(e, \dot{e}, q) + V_c(e, \dot{e}, q) \quad (54)$$

$$V_0(e, \dot{e}, q) = \frac{1}{2} \begin{bmatrix} e \\ \dot{e} \end{bmatrix}^T \begin{bmatrix} K_p & \mathbf{0} \\ \mathbf{0} & B^T A_e(q) D_e(q) B \end{bmatrix} \begin{bmatrix} e \\ \dot{e} \end{bmatrix} \quad (55)$$

$$V_c(e, \dot{e}, q) = \alpha(e) e^T B^T A_e(q) D_e(q) B \dot{e} \quad (56)$$

$$\alpha(e) = \frac{k_0}{1 + |e|} = \frac{k_0}{1 + \sqrt{e^T e}}. \quad (57)$$

It can be verified that V_e is positive definite. The addition of the cross terms V_c does not affect the positive definiteness as long as k_0 is sufficiently small. For example, we can pick k_0 that satisfies

$$k_0 \leq \frac{\sqrt{\|K_p\| \|B^T A_e D_e B\|}}{\|B^T A_e D_e B\|}. \quad (58)$$

Therefore, we can choose

$$k_0 = \frac{\sqrt{k_p}}{N}, \text{ where } N > \|B^T A_e D_e B\|^{\frac{1}{2}}. \quad (59)$$

We will be picking a larger value for N later on. Choosing this value of k_0 also helps in separating k_p from the positive definite matrix in (55) to obtain the following bounds on V_e :

$$\lambda_l \left\| \begin{bmatrix} \sqrt{k_p} e \\ \dot{e} \end{bmatrix} \right\|^2 \leq V_e \leq \lambda_u \left\| \begin{bmatrix} \sqrt{k_p} e \\ \dot{e} \end{bmatrix} \right\|^2, \quad (60)$$

for some positive constants λ_l, λ_u that do not depend on k_p . This type of inequality is useful for realizing desirable convergence rates for V_e (see [1, (10)-(22)] for a similar formulation).

V_e of the initial states. It is important to determine the sublevel sets of V_e that contains all the possible initial values. Since \mathcal{O}_z is locally stable in HZD, we can pick the same neighborhood radius r (or maybe even smaller) for the initial states (e_0, \dot{e}_0, z_0) . With this initial state we know from (50) and (51) that

$$|(e(0), \dot{e}(0))| \leq L_\Delta |(e_0, \dot{e}_0)| \leq L_\Delta r. \quad (61)$$

Therefore, given the initial state, the maximum possible value of V_e is $\lambda_u k_p L_\Delta^2 r^2$. This will be useful for determining the gains of the controller later on. We will now solve for the dynamics of V_e .

Derivative of V_0 . By solving for the derivative of V_0 , we get the following:

$$\dot{V}_0 = e^T K_p \dot{e} + \frac{1}{2} \dot{e}^T B^T (\dot{A}_e D_e + A_e \dot{D}_e) B \dot{e} + \dot{e}^T B^T A_e D_e B \ddot{e},$$

and after substituting (44) and (27) and using Propositions 3, 4, we have the final inequality as

$$\begin{aligned} \dot{V}_0 &= \frac{1}{2} \dot{e}^T B^T (\dot{A}_e D_e + A_e \dot{D}_e) B \dot{e} - \dot{e}^T B^T A_e (C_e \begin{bmatrix} \dot{z}_1 \\ \dot{e} \end{bmatrix} + G_e) \\ &\quad - k_p \dot{e}^T (B_e - \mathbf{1}) e - k_d \dot{e}^T B_e \dot{e} \\ &\leq \frac{c_u}{2} \left\| \begin{bmatrix} \dot{z}_1 \\ \dot{e} \end{bmatrix} \right\|^2 + c_u \left\| \begin{bmatrix} \dot{z}_1 \\ \dot{e} \end{bmatrix} \right\|^2 |\dot{e}| + c_u |\dot{e}| \\ &\quad - k_p \dot{e}^T (B_e - \mathbf{1}) e - k_d \dot{e}^T B_e \dot{e}. \end{aligned} \quad (62)$$

Derivative of V_c . By solving for the derivative of V_c , we have

$$\begin{aligned} \dot{V}_c &= \dot{\alpha} e^T B^T A_e D_e B \dot{e} + \alpha \dot{e}^T B^T A_e D_e B \dot{e} \\ &\quad + \alpha e^T B^T (\dot{A}_e D_e + A_e \dot{D}_e) B \dot{e} + \alpha e^T B^T A_e D_e B \ddot{e} \\ &\leq 2\alpha c_u |\dot{e}|^2 + \alpha c_u \left\| \begin{bmatrix} \dot{z}_1 \\ \dot{e} \end{bmatrix} \right\| |e| |\dot{e}| + \alpha c_u \left\| \begin{bmatrix} \dot{z}_1 \\ \dot{e} \end{bmatrix} \right\|^2 |e| + \alpha c_u |e| \\ &\quad - k_p \alpha e^T B_e e - k_d \alpha e^T B_e \dot{e}, \end{aligned} \quad (63)$$

where we have used Propositions 3, 4, and some of the properties of $\alpha(e)$:

$$\begin{aligned} |\alpha(e)| &\leq k_0, & |\alpha(e)| |e| &\leq k_0, \\ |\dot{\alpha}(e)| &\leq k_0 |\dot{e}|, & |\dot{\alpha}(e)| |e| &\leq k_0 |\dot{e}|. \end{aligned}$$

In addition, we note from (29), Property 2 and Assumptions 2, 3 that $B_e' \dot{z}_1 = D_{11}^{-1} (z_2 - D_{12} J^{-1} \dot{e})$, which yields

$$\left\| \begin{bmatrix} \dot{z}_1 \\ \dot{e} \end{bmatrix} \right\| \leq c_q \left\| \begin{bmatrix} z_2 \\ \dot{e} \end{bmatrix} \right\|, \quad (64)$$

for some $c_q > 0$. This can be substituted for \dot{z}_1, \dot{e} in the above equations. We obtain the total derivative as

$$\begin{aligned} \dot{V}_e &\leq -\frac{\alpha}{2} \begin{bmatrix} e \\ \dot{e} \end{bmatrix}^T \underbrace{\begin{bmatrix} k_p (B_e + B_e^T) & \frac{k_p (B_e^T - \mathbf{1}) + \alpha k_d B_e}{\alpha} \\ \frac{k_p (B_e - \mathbf{1}) + \alpha k_d B_e^T}{\alpha} & k_d (B_e + B_e^T) \end{bmatrix}}_{\Lambda} \begin{bmatrix} e \\ \dot{e} \end{bmatrix} \\ &\quad + \alpha c_u |z_2| |e| |\dot{e}| + c_u (\alpha |e| + |\dot{e}|) (|z_2|^2 + 1) \\ &\quad + 2c_u (\alpha + \alpha |e| + |\dot{e}| + |z_2|) |\dot{e}|^2, \end{aligned} \quad (65)$$

where c_u is redefined to absorb c_q . The control gains k_p, k_d must be picked in such a way that V_e is decreasing. For $|z_2|$,

we will pick the maximum of z in a compact neighborhood (tube) of \mathcal{O}_z . Assume that this maximum is $b > 0$ (say). Similarly, the maximum possible values for $|\dot{e}|, |e|$ in the sublevel set of V_e are given by

$$|\dot{e}| \leq \sqrt{k_p \frac{\lambda_u}{\lambda_l}} L_\Delta r =: |\dot{e}|_{\max}, |e| \leq \sqrt{\frac{\lambda_u}{\lambda_l}} L_\Delta r =: |e|_{\max}, \quad (66)$$

which are obtained from the maximum value of V_e for all possible initial states. Since $|\dot{e}|_{\max}$ depends on the proportional gain k_p , the derivative gain k_d must be at least as high as $\sqrt{k_p}$. Therefore, choose $k_p = \varepsilon^2, k_d = \varepsilon k, k_0 = \varepsilon/k$ for some $\varepsilon, k > 1$. We require that $\Lambda > 0$ i.e.,

$$\begin{bmatrix} e \\ \dot{e} \end{bmatrix}^T \Lambda \begin{bmatrix} e \\ \dot{e} \end{bmatrix} = \begin{bmatrix} \varepsilon e \\ k \dot{e} \end{bmatrix}^T \Lambda_{B_e} \begin{bmatrix} \varepsilon e \\ k \dot{e} \end{bmatrix} > 0, \quad (67)$$

for all $(q, \dot{q}) \in \cup_{q \in \mathbb{N}_r} T_q \mathcal{Q}$. This is true by Assumption 3. Therefore, we have the following:

$$\begin{aligned} \dot{V}_e \leq & -\frac{\alpha}{2} \lambda_{B_e} \left\| \begin{bmatrix} \varepsilon e \\ k \dot{e} \end{bmatrix} \right\|^2 + \alpha k_1 |e| |\dot{e}| + \alpha k_2 |\dot{e}|^2 \\ & + k_3 (\alpha |e| + |\dot{e}|), \end{aligned} \quad (68)$$

where $\lambda_{B_e} := \lambda_{\min}(\Lambda_{B_e})$ is the minimum eigenvalue in the compact set \mathbb{N}_r , and

$$\begin{aligned} k_1(|z_2|) &= c_u |z_2| \\ k_2(|e|, |\dot{e}|, |z_2|) &= 2c_u \left(1 + |e| + \frac{(|\dot{e}| + |z_2|)}{\varepsilon k^{-1}(1 + |e|)^{-1}} \right) \\ k_3(|z_2|) &= c_u (|z_2|^2 + 1). \end{aligned} \quad (69)$$

One half of the first summand in (68) can be used to cancel the next two summands in the following manner:

$$\begin{aligned} -\frac{\lambda_{B_e}}{4} |(\varepsilon e, k \dot{e})|^2 + k_1 |e| |\dot{e}| + k_2 |\dot{e}|^2 = \\ - \begin{bmatrix} |e| \\ |\dot{e}| \end{bmatrix}^T \begin{bmatrix} \frac{\varepsilon^2 \lambda_{B_e}}{4} & -k_1 \\ -k_1 & \frac{k^2 \lambda_{B_e}}{4} - k_2 \end{bmatrix} \begin{bmatrix} |e| \\ |\dot{e}| \end{bmatrix}, \end{aligned} \quad (70)$$

where the summands are collected together in the form of a matrix. We can replace e, \dot{e}, z_2 in k_1, k_2 with their maximum possible values, and by choosing a large enough k , we can ensure that (70) is negative.

Note that (70) is satisfied even if ε is increased ($|\dot{e}| \leq |\dot{e}|_{\max}$ is canceled by ε in the denominator in (69)), and if the k chosen does not satisfy (58) i.e., if $k \not\geq N$, then we simply increase it further. We will be using ε as a tunable gain for

obtaining desirable convergence rates. We have that

$$\begin{aligned} \dot{V}_e &\leq -\frac{\alpha \lambda_{B_e}}{4} |(\varepsilon e, k \dot{e})|^2 + k_3 (\alpha |e| + |\dot{e}|) \\ &\leq -\frac{\alpha \lambda_{B_e}}{8} |(\varepsilon e, \dot{e})|^2 + \frac{2\alpha k_3^2}{\lambda_{B_e} \varepsilon^2} + \frac{2k_3^2 k^2}{\lambda_{B_e} \alpha} \\ &\leq -2\varepsilon \lambda V_e + \frac{2\alpha k_3^2}{\lambda_{B_e} \varepsilon^2} + \frac{2k_3^2 k^2}{\lambda_{B_e} \alpha}, \end{aligned} \quad (71)$$

where $\lambda := \lambda_{B_e} / (16k(1 + |\dot{e}|_{\max})\lambda_u)$. The above inequality is satisfied as long as z remains in the tube. Let T_δ be the time when z crosses this limit. Therefore, by using comparison lemma [16, Lemma 3.4] in (71), we have that

$$V_e(t) \leq e^{-2\varepsilon \lambda t} V_e(0) + \frac{k_4}{\varepsilon^2}, \quad t \in [0, T_\delta], \quad (72)$$

where k_4 is obtained by collecting all the additional terms that are independent of ε . We can express the above inequality in terms of the outputs as

$$\begin{aligned} \left\| \begin{bmatrix} e(t) \\ \dot{e}(t) \end{bmatrix} \right\|^2 &\leq \varepsilon^2 e^{-2\varepsilon \lambda t} \frac{\lambda_u}{\lambda_l} \left\| \begin{bmatrix} e(0) \\ \dot{e}(0) \end{bmatrix} \right\|^2 + \frac{k_4}{\varepsilon^2 \lambda_l} \\ \left\| \begin{bmatrix} e(t) \\ \dot{e}(t) \end{bmatrix} \right\| &\leq \varepsilon e^{-\varepsilon \lambda t} \sqrt{\frac{\lambda_u}{\lambda_l}} \left\| \begin{bmatrix} e(0) \\ \dot{e}(0) \end{bmatrix} \right\| + \sqrt{\frac{k_4}{\varepsilon^2 \lambda_l}}, \end{aligned} \quad (73)$$

which completes the proof.

Remark 4 We showed that increasing ε increases the convergence rate of the outputs. It is important to note that this also results in changing shape of the Lyapunov level sets of V_e . The peak velocity $|\dot{e}|_{\max}$ increases with increasing ε . On the other hand, increasing ε does not increase $|e|_{\max}$. Therefore, Assumptions 2 and 3 are still valid. We will now prove Lemma 2.

PROOF. [of Lemma 2] Firstly, we note that by the differentiability of Φ (diffeomorphism):

$$|q(t) - q^*(t)| \leq L_q (|z_1(t) - z_1^*(t)| + |e(t)|), \quad (74)$$

where L_q is the local Lipschitz constant (for the tube of radius r around the orbit). By using the definition of the zero coordinates, we have that

$$\begin{aligned} \dot{z}_1(t) - \dot{z}_1^*(t) &= B_e'(q(t))^{-1} D_{11}(q(t))^{-1} [z_2(t) \\ &\quad - D_{12}(q(t)) J(q(t))^{-1} \dot{e}(t)] \\ &\quad - B_e'(q^*(t))^{-1} D_{11}(q^*(t))^{-1} z_2^*(t). \end{aligned} \quad (75)$$

Here B_e' is given by (43), and $q^*(t), z_1^*(t)$ correspond to the trajectory on \mathcal{O} . By collecting the common terms, we obtain

the following inequality:

$$|\dot{z}_1(t) - \dot{z}_1^*(t)| \leq c_z(|z_2(t) - z_2^*(t)| + |q(t) - q^*(t)| + |\dot{e}(t)|), \quad (76)$$

for some $c_z > 0$. We can have a similar inequality for the derivative of $z_2(t) - z_2^*(t)$:

$$|\dot{z}_2(t) - \dot{z}_2^*(t)| \leq c_z(|\dot{z}_1(t) - \dot{z}_1^*(t)| + |\dot{z}_1(t) - \dot{z}_1^*(t)|^2 + |\dot{e}(t)| + |\dot{e}(t)|^2 + |q(t) - q^*(t)|), \quad (77)$$

for, perhaps, a larger value for $c_z > 0$. By using (74), (76) and (77), we establish that

$$|\dot{z}(t) - \dot{z}^*(t)| \leq c_z \left(\left\| \begin{bmatrix} z(t) - z^*(t) \\ \eta(t) \end{bmatrix} \right\| + \left\| \begin{bmatrix} z(t) - z^*(t) \\ \eta(t) \end{bmatrix} \right\|^2 \right), \quad (78)$$

for some $c_z > 0$ (possibly larger than the previously determined c_z). We have used $\eta(t) := (e(t), \dot{e}(t))$ for convenience. We substitute (78) in the following inequality:

$$\begin{aligned} |z(t) - z^*(t)| &\leq |z(0) - z^*(0)| + \int_0^t |\dot{z}(s) - \dot{z}^*(s)| ds \\ &\leq |z(0) - z^*(0)| + c_z \int_0^t (|\eta(s)| + |\eta(s)|^2) ds \\ &\quad + c_z \int_0^t (|z(s) - z^*(s)| + |z(s) - z^*(s)|^2) ds. \end{aligned}$$

For a tube of radius r around \mathcal{O}_z , we have that $|z(t)|, |z^*(t)| \leq b$. Therefore, by substituting b and the expression for the outputs $\eta(t)$, we have that

$$\begin{aligned} |z(t) - z^*(t)| &\leq |z(0) - z^*(0)| + \frac{c_z \varepsilon \lambda_u}{2\lambda_l} |\eta(0)|^2 + \frac{c_z k_4 T_\delta}{\varepsilon^2 \lambda_l} \\ &\quad + \frac{c_z}{\lambda} \sqrt{\frac{\lambda_u}{\lambda_l}} |\eta(0)| + c_z \sqrt{\frac{k_4}{\varepsilon^2 \lambda_l}} T_\delta \\ &\quad + c_z (1 + 2b) \int_0^t |z(s) - z^*(s)| dt. \end{aligned} \quad (79)$$

By using Gronwall-Bellman inequality [16, Lemma A.1], we obtain

$$|z(t) - z^*(t)| \leq c_z \left(|z_0| + \varepsilon |\eta_0|^2 + |\eta_0| + \frac{T_\delta}{\varepsilon^2} + \frac{T_\delta}{\varepsilon} \right) e^{c_z(1+2b)t}, \quad (80)$$

where the pre-impact state (η_0, z_0) is substituted and c_z is appropriately redefined. We establish the first part of Lemma 2 by substituting $z_0 = z^* = 0$, $\eta_0 = 0$ and appropriately choosing C_k, C_l .

To establish the second part of Lemma 2, we first note that the constant terms in (80) decrease with increasing ε . Therefore, $z(t)$ gets closer to \mathcal{O} with decreasing r and increasing

ε , implying that the states are bounded for $[0, T_\delta]$. Since T_δ is the time when $|z_2(t)|$ crosses its bound b , i.e., leaves the compact neighborhood around \mathcal{O}_z , we can use the steps followed in [16, Theorem 3.5]. T_δ is stretched to an arbitrary constant $T_\delta = T_{\max} > T^*$ (say), and by choosing ε (say ε_1), and r (say r_1 that is smaller than previously chosen), we ensure that Lemma 1 is valid for the entire $[0, T_{\max}]$. With this result, the next steps are similar to [35, Proof of Lemma 2], where we use implicit function theorem (in function spaces) to establish bounds for the time-to-impact function (45). We know that on the nominal orbit, we obtain the period T^* as

$$T^* = \inf\{t > 0 : h(\Phi^{-1}(0, 0, z^*(t))) = 0\}, \quad (81)$$

which is well defined. By transversality condition (see [35, A.7]), any small perturbation of the trajectories from the nominal orbit in the guard function $h(\Phi^{-1}(\mu_1(t), 0, z^*(t) + \mu_2(t)))$ will still yield a well defined time-to-impact function, as long as the perturbations $\mu_1(t), \mu_2(t)$ are small⁴. Pick $\mu_1(t) = e(t)$, $\mu_2(t) = z(t) - z^*(t)$, and the resulting guard function yields (45). We can quantify μ_i 's by using function norms. Denote the functional norms as

$$\begin{aligned} \|e\|_\infty &:= \sup_{t \in [0, T_{\max}]} |e(t)| \\ \|z - z^*\|_\infty &:= \sup_{t \in [0, T_{\max}]} |z(t) - z^*(t)|. \end{aligned} \quad (82)$$

Both $\|e\|_\infty$ and $\|z - z^*\|_\infty$ can be evaluated from (73) and (80) respectively. Since the initial state is $(0, 0, z^*)$, we know that by increasing ε , $\|e\|_\infty$ and $\|z - z^*\|_\infty$ can be decreased. Given $\delta > 0$, if $\delta > T_{\max} - T^*$, we will first pick a smaller $\delta_1 > 0$ that ensures that $T^* + \delta_1 < T_{\max}$. Therefore, given $\delta_1 > 0$, we can obtain a larger $\varepsilon > \varepsilon_1$ (say ε_2) such that (47) is satisfied.

We will now establish the third part of Lemma 2. Similar to T_{\max} , we can manually set some $T_{\min} > 0$ such that $T_{\min} < T^* < T_{\max}$ ⁵. We choose $\delta < \min\{T_{\max} - T^*, T^* - T_{\min}\}$, and the corresponding time-to-impact satisfies $T_{\min} < T(0, 0, z^*) < T_{\max}$, for $\varepsilon \geq \varepsilon_2$. Note that ε can be increased even further to decrease the bound on e, z . Accordingly, we can choose a small enough neighborhood (smaller than r_1) around $(0, 0, z^*)$ in such a way that (48) is satisfied, while still satisfying the conditions of implicit function theorem and boundedness of $z(t)$. This completes the proof.

Remark 5 For the initial state $(0, 0, z^*)$, we have that $\varepsilon \rightarrow \infty \implies$ the resulting evolution of $z(t)$ is identically equal to $z^*(t)$. For the non-zero initial state (e_0, \dot{e}_0, z_0) , it can be verified that the norm $\|z - z^*\|_\infty$ does not increase with increasing ε if the neighborhood radius r is chosen appropriately. For example, we can choose r such that it is inversely proportional to $\sqrt{\varepsilon}$ (see (80)). In addition, the peak value of

⁴ h is not dependent on velocity \dot{e} , and hence the second argument being zero still yields the time-to-impact function.

⁵ In [1, Lemma 1], T_{\min}, T_{\max} were chosen to be $0.9T^*, 1.1T^*$ respectively.

$|e(t)|$ only depends on r (see (66)). This will be useful for increasing ε to arbitrarily large values later on. We will now prove Lemma 3.

PROOF. [of Lemma 3] We will first study the progression of $\eta(t)$ till the end of the step $t = T$. By replacing T with its extreme values T_{\min}, T_{\max} , we have the following from (73):

$$|\eta(T)| \leq \beta(\varepsilon)|\eta| + d_\eta(\varepsilon), \quad (83)$$

where the subscript 0 was omitted for convenience, and

$$\beta(\varepsilon) = \sqrt{\frac{\lambda_u}{\lambda_l}} \varepsilon e^{-\varepsilon \lambda T_{\min}}, \quad d_\eta(\varepsilon) = \sqrt{\frac{k_4}{\varepsilon^2 \lambda_l}}. \quad (84)$$

Here the dependency of β, d_η on ε is explicitly shown. Note that β has an upper bound (denote it by $\bar{\beta}$) that is independent of ε .

We can obtain similar inequalities for the zero coordinates. Firstly, we know that $z(t)$ is the trajectory of the zero coordinate on the full order hybrid dynamics (39) with the initial condition (η, z) on the guard, and $z_s(t)$ is the trajectory on the HZD with the initial condition z on the guard. For a fixed $\varepsilon \geq \varepsilon_2$, we know that we can pick an r (see Remark 5) in such a way that

$$|z(T) - z_s(T)| \leq C_z |\eta| + d_z(\varepsilon), \quad (85)$$

where C_z, d_z are both obtained by collecting all the terms together. This is similar to the inequality (80). The rest of the steps are very similar to [1, Proof of Lemma 1]. We define an auxiliary time-to-impact function:

$$T_B(\mu_\eta, \mu_z, z) = \inf_{t > 0} \{t : h(\Phi^{-1}(\mu_\eta, z_s(t) + \mu_z)) = 0\}, \quad (86)$$

where $\mu_\eta \in \mathbb{R}^{2m}$, $\mu_z \in \mathbb{R}^{2l}$, and satisfies

$$|T_B(\mu_\eta, \mu_z, z) - T_\rho(z)| \leq L_B(|\mu_\eta| + |\mu_z|), \quad (87)$$

where L_B is the Lipschitz constant. In addition, μ_η, μ_z are further defined to be

$$\mu_\eta = \eta(t)|_{t=T(\eta, z)}, \quad \mu_z = z(t) - z_s(t)|_{t=T(\eta, z)}, \quad (88)$$

which yields $T_B(\mu_\eta, \mu_z, z) = T(\eta, z)$. With this result, and by substituting (83), (85), and also the bound on $\beta(\varepsilon)$ in (87), we get the first result (52).

The second result (53) will follow exactly the steps in [1, Proof of Lemma 1] with the substitution of (52). Define

$$C_\psi = \max_{T_{\min} \leq t \leq T_{\max}} |\psi(0, z_s(t))|. \quad (89)$$

We therefore have

$$\begin{aligned} |\mathbb{P}_z(\eta, z) - \rho(z)| &\leq |z(0) - z_s(0) + \\ &\quad \int_0^{T(\eta, z)} \psi(\eta(t), z(t)) - \psi(0, z_s(t)) dt| \\ &\quad + \left| \int_{T(\eta, z)}^{T_\rho(z)} \psi(0, z_s(t)) dt \right|. \end{aligned} \quad (90)$$

The first two terms on the RHS are substituted with (85), and the last term can be replaced with (89) and (52). This completes the proof.

We are now ready to prove the main theorem.

PROOF. [of Theorem 2] Since we know that exponential stability of \mathcal{O}_z yields a discrete time Lyapunov function $V_z(z)$ (37), we need to construct a suitable Lyapunov function for the full order system.

Lyapunov candidate for \mathbb{P} : Consider the following Lyapunov candidate for the Poincaré map:

$$V(\eta, z) = \sigma |\eta|^2 + V_z(z), \quad (91)$$

where $\sigma > 0$ is a tunable constant, and (η, z) is the initial state (by a slight abuse of notations).

We will analyze the two terms in RHS of (91) separately. We note in (83) that $\beta(\varepsilon)$ can be reduced by increasing ε . Hence, we can obtain $\bar{\varepsilon} > \varepsilon_2$ in such a way that $\beta(\varepsilon) < 1/2$ (say) for all $\varepsilon \geq \bar{\varepsilon}$. We may have to increase ε further to decrease the ultimate bound later on. We have

$$|\mathbb{P}_\eta(\eta, z)|^2 - |\eta|^2 \leq -(1 - \beta(\varepsilon)^2) |\eta|^2 + d_\eta(\varepsilon)^2. \quad (92)$$

By using (37), we have the following:

$$\begin{aligned} V_z(\mathbb{P}_z(\eta, z)) - V_z(z) &= V_z(\mathbb{P}_z(\eta, z)) - V_z(\rho(z)) + V_z(\rho(z)) - V_z(z) \\ &\leq c_4 |\mathbb{P}_z(\eta, z) - \rho(z)| \cdot (|\mathbb{P}_z(\eta, z)| + |\rho(z)|) - c_3 |z|^2 \\ &\leq -c_3 |z|^2 + c_4 (C_\rho |\eta| + d_\rho(\varepsilon))^2 \\ &\quad + c_4 (L_\rho + c_5 \gamma) (C_\rho |\eta| + d_\rho(\varepsilon)) |z|, \end{aligned} \quad (93)$$

where L_ρ is the Lipschitz constant of ρ . The remaining steps are similar to [23, Eqns. (92)-(94)], which yields

$$V(\mathbb{P}(\eta, z)) - V(\eta, z) \leq - \begin{bmatrix} |\eta| \\ |z| \end{bmatrix}^T \Lambda_{\mathcal{H}} \begin{bmatrix} |\eta| \\ |z| \end{bmatrix} + d(\sigma, \varepsilon), \quad (94)$$

where

$$\Lambda_{\mathcal{H}} = \begin{bmatrix} \sigma \frac{1-2\beta(\varepsilon)^2}{2} - c_4 C_P^2 & -\frac{c_4 C_P (L_P + c_5 \gamma)}{2} \\ -\frac{c_4 C_P (L_P + c_5 \gamma)}{2} & \frac{c_3}{2} \end{bmatrix} \quad (95)$$

$$d(\sigma, \varepsilon) = \sigma d_{\eta}(\varepsilon)^2 + \left[\frac{2C_P^2}{\sigma} + \frac{1}{c_4} + \frac{(L_P + c_5 \gamma)^2}{2c_3} \right] c_4^2 d_P(\varepsilon)^2.$$

By choosing a large enough σ , it can be verified that $\Lambda_{\mathcal{H}}$ is positive definite. We complete the proof by picking an even larger $\varepsilon > \bar{\varepsilon}$ such that $d(\sigma, \varepsilon)$ is sufficiently small.

6 Results

In this section we will discuss simulation results on a 2-link walker platform shown in Fig. 2. The biped is planar with 2 links; this model was primarily used to establish robust walking behaviors in [27]. The robot has point feet, and is thus underactuated at the ankle. Table 2 provides the list of physical parameters of the 2-link walker. More details about this model are found in [27].

Outputs and control. We have the configuration as $q = (q_1, q_2)$, where q_1 is the angle between the legs i.e., angle between the stance and nonstance legs, q_2 is the stance leg angle w.r.t. the vertical axis. The output is defined as follows:

$$e(q) = q_1 - q_d^a(\tau(q_2)), \quad (96)$$

where q_d^a is a 5th order polynomial:

$$q_d^a(\tau) = \sum_{j=0}^5 \zeta_j \tau^{5-j} (1-\tau)^j, \quad \tau(q_2) = \frac{q_2 - q_0}{q_f - q_0}, \quad (97)$$

with ζ_j 's being the parameters 0.5753, 3.1632, 0.3115, -0.0570, -1.9988, -0.5753 in increasing order, and q_0, q_f being the initial and final values of q_2 on the orbit. These parameters are obtained via an offline optimization problem [11,39,40]. The control law is given by (27). We chose the following gain values, and then studied the resulting walking:

$$k_p = \varepsilon^2, \quad k_d = \varepsilon k, \quad \text{with } \varepsilon = 5, 10, 20, \quad k = 2. \quad (98)$$

$\varepsilon = 5$ resulted in eventual falling, while $\varepsilon = 10, 20$ resulted in stable walking. We verified that Assumption 3 was satisfied throughout the step, which is shown in Fig. 3. Fig. 4 shows the responses and torque profiles for these different gains. Fig. 5 shows the phase portrait of the zero coordinates for 100 steps for $\varepsilon = 20, 40$. It can be verified from Figs. 4 and 5 that increasing ε not only increases the convergence rate, but also reduces the ultimate bound.

Model Parameters			
Link	Mass (kg)	Length l (m)	Center l_c (m)
Leg	0.103	0.5	0.33
Hip	0.068	N/A	0

Table 2

The table of parameters for the 2-link walker is shown here.

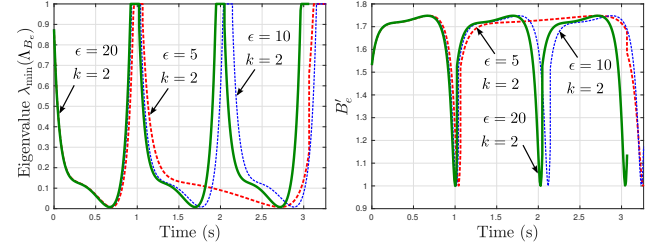


Fig. 3. Left figure is showing the minimum eigenvalue of Λ_{B_e} (see Assumption 3), and the right figure is showing B'_e for three steps. This shows that Assumption 3 is valid for the gait obtained.

7 Conclusions

We established that PD control laws are sufficient to realize locally stable periodic orbits in underactuated hybrid robotic systems. As an example, we have realized stable walking in a 2-link bipedal walker. The key methodology is to use derivative gains that are at least as high as the square root of the proportional gains, and then increase the proportional gains as high as possible. It is important to note that properties like existence of stable periodic orbits in HZD, and low variations of the desired trajectories w.r.t. the unactuated coordinates have been used to achieve stable walking. We are also assuming that the joint actuators have high torque limits. These are not restrictive, and can be used as guidelines for the biped design process.

Acknowledgements

The author would like to acknowledge Sushant Veer and Wen-Loong Ma for providing useful insights and suggestions in improving the proofs in the paper.

A Proofs of Propositions 1 and 2

PROOF. For convenience let $D_s(q) := B^T A(q) D(q) B$. It is easy to see why D_s is symmetric. By [3, A.5.5], D_s is positive definite. We consider the inverse of D , which is obtained as

$$D^{-1} = \begin{bmatrix} D_{11}^{-1} + D_{11}^{-1} D_{12} D_s^{-1} D_{21} D_{11}^{-1} & -D_{11}^{-1} D_{12} D_s^{-1} \\ -D_s^{-1} D_{21} D_{11}^{-1} & D_s^{-1} \end{bmatrix}. \quad (\text{A.1})$$

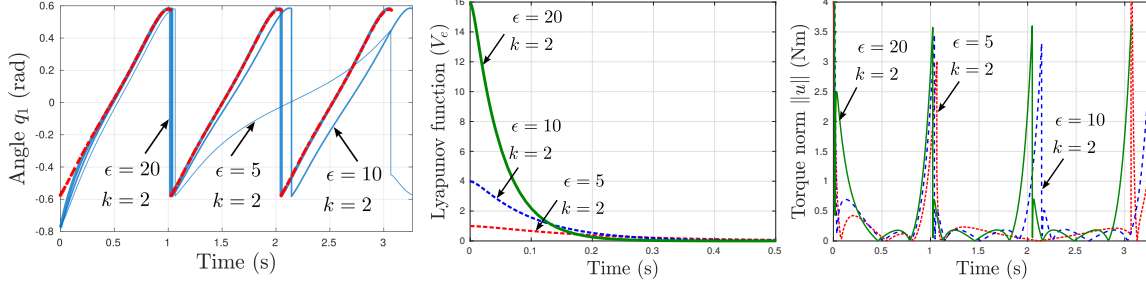


Fig. 4. Left figure is showing the comparison between the actual and nominal (dashed) trajectories for different gains of the control law (27). The center figure is showing the Lyapunov functions varying as a function of time. The right figure is showing the corresponding torque values varying as a function of time. Since the Lyapunov functions are decaying fast, their plots are shown for a shorter duration. Note that the nominal trajectories are not the same as the desired trajectories.

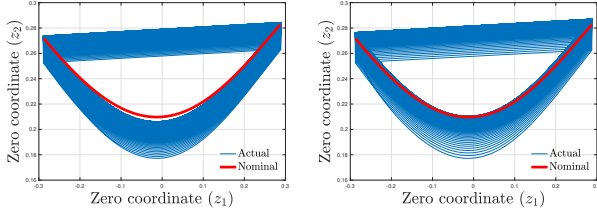


Fig. 5. Figure showing the phase portrait of the zero coordinates for $\epsilon = 20$ (left) and for $\epsilon = 40$ (right). The phase portrait for the nominal gait is shown for reference. The thick band indicates the region where the walking trajectories are mostly lying. The band is thinner and closer to the nominal curve for $\epsilon = 40$.

Since $\|D^{-1}\|$ has upper and lower bounds (eigenvalues of D^{-1} are the inverse eigenvalues of D), D_s must have upper and lower bounds. We will choose these bounds to be c_l, c_u respectively. The rest of the properties can be obtained directly from Property 2 (since D contains only sine and cosine functions of q , their derivatives are bounded w.r.t. q).

B Proof of Proposition 3

PROOF. Positive definiteness of D_e , and skew symmetry of $\dot{D}_e - 2C_e$ are shown in [30, Lemma 4.11]. To prove the second part of the proposition, we have that

$$\|D_e\| \leq \|J_e^{-T}\| \|D\| \|J_e^{-1}\|, \quad (\text{B.1})$$

and based on boundedness and invertibility of J_e , we choose a c_u (possibly larger) that bounds D_e . Similarly

$$\|D\| \leq \|J_e^T\| \|D_e\| \|J_e\|, \quad (\text{B.2})$$

and the lower bound can be obtained accordingly. Similar procedure follows for D_e^{-1}, G_e . For \dot{D}_e we have

$$\|\dot{D}_e\| = \left\| \frac{\partial D_e}{\partial q} J_e^{-1} \begin{bmatrix} \dot{q}^u \\ \dot{e} \end{bmatrix} \right\| \leq c_u (|\dot{q}^u| + |\dot{e}|), \quad (\text{B.3})$$

for some $c_u > 0$. Similar procedure follows for C_e .

C Proof of Proposition 4

PROOF. Proof is very similar to Proof of Propositions 1, 2, and 3. We note that A_e, D_e are purely functions of the configuration q from a compact space \mathbb{N} . Therefore, the arguments follow directly from (A.1), (B.1), (B.2), (B.3).

References

- [1] A. D. Ames, K. Galloway, K. Sreenath, and J. W. Grizzle. Rapidly exponentially stabilizing control Lyapunov functions and hybrid zero dynamics. *IEEE Transactions on Automatic Control*, 59(4):876–891, 2014.
- [2] S. Arimoto and F. Miyazaki. Asymptotic stability of feedback control laws for robot manipulator. *IFAC Proceedings Volumes*, 18(16):221–226, 1985. 1st IFAC Symposium on Robot Control.
- [3] S. Boyd and L. Vandenberghe. *Convex optimization*. Cambridge university press, 2004.
- [4] S. Brakken-Thal. Gershgorins theorem for estimating eigenvalues. 2007.
- [5] Y. Choi and W. K. Chung. *PID trajectory tracking control for mechanical systems*, volume 298. Springer, 2004.
- [6] F. Ghorbel, B. Srinivasan, and M. W. Spong. On the uniform boundedness of the inertia matrix of serial robot manipulators. *Journal of Robotic Systems*, 15(1):17–28, 1998.
- [7] J. W. Grizzle, Christine Chevallereau, Aaron D. Ames, and Ryan W. Sinnet. 3d bipedal robotic walking: Models, feedback control, and open problems. *IFAC Proceedings Volumes*, 43(14):505–532, 2010.
- [8] J. W. Grizzle, J. Hurst, B. Morris, H. Park, and K. Sreenath. MABEL, a new robotic bipedal walker and runner. In *American Control Conference*, pages 2030–2036, St. Louis, MO, USA, 2009.
- [9] R. Gunawardana and F. Ghorbel. The class of robot manipulators with bounded jacobian of the gravity vector. In *Proceedings of IEEE International Conference on Robotics and Automation*, volume 4, pages 3677–3682 vol.4, April 1996.
- [10] K. A. Hamed, B. G. Buss, and J. W. Grizzle. Exponentially stabilizing continuous-time controllers for periodic orbits of hybrid systems: Application to bipedal locomotion with ground height variations. *The International Journal of Robotics Research*, 35(8):977–999, 2016.
- [11] A. Hereid, E. A. Cousineau, C. M. Hubicki, and A. D. Ames. 3d dynamic walking with underactuated humanoid robots: A direct collocation framework for optimizing hybrid zero dynamics. In *2016 IEEE International Conference on Robotics and Automation (ICRA)*, pages 1447–1454, 5 2016.

- [12] C. Hubicki, J. Grimes, M. Jones, D. Renjewski, A. Spröwitz, A. Abate, and J. Hurst. Atrias: Design and validation of a tether-free 3D-capable spring-mass bipedal robot. *The International Journal of Robotics Research*, 2016.
- [13] Y. Hurmuzlu. Dynamics of bipedal gait; part i: Objective functions and the contact event of a planar five-link biped. *ASME Journal of Applied Mechanics*, 60(2):331–336, 1993.
- [14] Y. Hurmuzlu and D. B. Marghitu. Rigid body collisions of planar kinematic chains with multiple contact points. *The International Journal of Robotics Research*, 13(1):82–92, 1994.
- [15] S. Kawamura, F. Miyazaki, and S. Arimoto. Is a local linear pd feedback control law effective for trajectory tracking of robot motion? In *Proceedings of IEEE International Conference on Robotics and Automation*, pages 1335–1340 vol.3, April 1988.
- [16] H. K. Khalil. *Nonlinear systems*, volume 3. Prentice hall Upper Saddle River, NJ, 2002.
- [17] D. E. Koditschek. Natural motion for robot arms. In *Proceedings of IEEE Conference on Decision and Control*, volume 23, pages 733–735. IEEE, 1984.
- [18] D. E. Koditschek. Adaptive techniques for mechanical systems. In *Fifth Yale Workshop on Applications of Adaptive Systems Theory*, May 1987, pages 259–265, 1987.
- [19] D. E. Koditschek. High gain feedback and telerobotic tracking. In *Proceedings of the Workshop on Space Telerobotics*, pages 355–363, 1987.
- [20] D. E. Koditschek. Strict global lyapunov functions for mechanical systems. In *Proceedings of American Control Conference*, pages 1770–1775, June 1988.
- [21] D. E. Koditschek. Robot planning and control via potential functions. pages 349–367, 1989.
- [22] S. Kolathaya and A. D. Ames. Parameter sensitivity and boundedness of robotic hybrid periodic orbits. *IFAC-PapersOnLine*, 48(27):377 – 382, 2015.
- [23] S. Kolathaya and A. D. Ames. Parameter to state stability of control Lyapunov functions for hybrid system models of robots. *Nonlinear Analysis: Hybrid Systems*, 25:174 – 191, 2017.
- [24] S. Kolathaya, A. Hereid, and A. D. Ames. Time dependent control Lyapunov functions and hybrid zero dynamics for stable robotic locomotion. In *2016 American Control Conference (ACC)*, pages 3916–3921, 7 2016.
- [25] T-T. Lu and S-H. Shiou. Inverses of 2×2 block matrices. *Computers & Mathematics with Applications*, 43(1):119 – 129, 2002.
- [26] W-L. Ma, S. Kolathaya, E. R. Ambrose, C. M. Hubicki, and A. D. Ames. Bipedal robotic running with DURUS-2D: Bridging the gap between theory and experiment. In *Proceedings of the 20th International Conference on Hybrid Systems: Computation and Control*, HSCC '17, pages 265–274, NY, USA, 2017. ACM.
- [27] I. R. Manchester, U. Mettin, F. Iida, and R. Tedrake. Stable dynamic walking over uneven terrain. *The International Journal of Robotics Research*, 30(3):265–279, 2011.
- [28] B. Morris and J. W. Grizzle. A restricted Poincaré map for determining exponentially stable periodic orbits in systems with impulse effects: Application to bipedal robots. In *IEEE Conf. on Decision and Control*, Seville, Spain, 2005.
- [29] J. I. Mulero-Martinez. Uniform bounds of the Coriolis/centripetal matrix of serial robot manipulators. *Robotics, IEEE Transactions on*, 23(5):1083–1089, 10 2007.
- [30] R. M. Murray, Zexiang Li, and S. S. Sastry. *A Mathematical Introduction to Robotic Manipulation*. CRC Press, Boca Raton, 1994.
- [31] M. Posa, C. Cantu, and R. Tedrake. A direct method for trajectory optimization of rigid bodies through contact. *The International Journal of Robotics Research*, 33(1):69–81, 2014.
- [32] J. P. Reher, A. Hereid, S. Kolathaya, C. M. Hubicki, and A. D. Ames. *Algorithmic Foundations of Realizing Multi-Contact Locomotion on the Humanoid Robot DURUS*. Springer Berlin Heidelberg, Berlin, Heidelberg, 2017.
- [33] T. Samad. A survey on industry impact and challenges thereof [technical activities]. *IEEE Control Systems*, 37(1):17–18, Feb 2017.
- [34] M. Takegaki and S. Arimoto. A New Feedback Method for Dynamic Control of Manipulators. *Journal of Dynamic Systems Measurement and Control-transactions of The Asme*, 103, 1981.
- [35] S. Veer, Rakesh, and I. Poulakakis. Input-to-state stability of periodic orbits of systems with impulse effects via poincaré analysis. *IEEE Transactions on Automatic Control*, 64(11):4583–4598, Nov 2019.
- [36] J. T. Wen and D. S. Bayard. New class of control laws for robotic manipulators part 1. non-adaptive case. *International Journal of Control*, 47(5):1361–1385, 1988.
- [37] E. R. Westervelt, J. W. Grizzle, and D. E. Koditschek. Hybrid zero dynamics of planar biped walkers. *IEEE Transactions on Automatic Control*, 48(1):42–56, 2003.
- [38] L. L. Whitcomb, A. A. Rizzi, and D. E. Koditschek. Comparative experiments with a new adaptive controller for robot arms. *IEEE Transactions on Robotics and Automation*, 9(1):59–70, Feb 1993.
- [39] S. N. Yadukumar, M. Pasupuleti, and A. D. Ames. Human-inspired underactuated bipedal robotic walking with AMBER on flat-ground, up-slope and uneven terrain. In *2012 IEEE/RSJ International Conference on Intelligent Robots and Systems*, pages 2478–2483, October 2012.
- [40] S. N. Yadukumar, M. Pasupuleti, and A. D. Ames. *From Formal Methods to Algorithmic Implementation of Human Inspired Control on Bipedal Robots*, pages 511–526. Springer Berlin Heidelberg, Berlin, Heidelberg, 2013.



Shishir Kolathaya is an INSPIRE Faculty Fellow in the Robert Bosch Center for Cyber Physical Systems at the Indian Institute of Science, Bengaluru, India. Previously, he was a Postdoctoral Scholar in the department of Mechanical and Civil Engineering at the California Institute of Technology. He received his Ph.D. degree in Mechanical Engineering (2016) from the Georgia Institute of Technology, his M.S. degree in Electrical Engineering (2012) from Texas A&M University, and his B. Tech. degree in Electrical & Electronics Engineering (2008) from the National Institute of Technology Karnataka, Surathkal. Shishir is interested in stability and control of nonlinear hybrid systems, especially in the domain of legged robots. His more recent work is also focused on real-time safety-critical control for robotic systems.